

## Electronic Supplementary Information

### **Assembly of Discrete and Oligomeric Structures of Organotin Double-decker Silsesquioxanes: Inherent Stability Studies**

Pushparaj Loganathan,<sup>a</sup> Renjith S. Pillai,<sup>a,b</sup> Velusamy Jeevananthan,<sup>a</sup> Ezhumalai David,<sup>c</sup>  
Nallasamy Palanisami,<sup>c</sup> Nattamai S. P. Bhuvanesh,<sup>d</sup> and Swaminathan Shanmugan<sup>\*a</sup>

<sup>a</sup>Department of Chemistry, Faculty of Engineering and Technology, SRM Institute of Science and Technology, Kattankulathur-603203, Tamil Nadu, India.

<sup>b</sup>Department of Chemistry, Christ University, Bangalore-56029, Karnataka, India.

<sup>c</sup>Centre for Functional Materials, Department of Chemistry, School of Advanced Sciences, Vellore Institute of Technology, Vellore-632014, Tamil Nadu, India.

<sup>d</sup>X-ray Diffraction Laboratory, Department of Chemistry, Texas A&M University, College Station, TX 77842, USA.

Corresponding author: Swaminathan Shanmugan ([shanmugs2@srmist.edu.in](mailto:shanmugs2@srmist.edu.in),  
[shanmugan0408@gmail.com](mailto:shanmugan0408@gmail.com))

## Contents

**Figure S1.** FT-IR spectra of DDSQ-4OH, compound **1** and **2**.

**Figure S2.**  $^1\text{H}$  NMR spectrum of compound **1**.

**Figure S3.**  $^1\text{H}$  NMR spectrum of compound **2**.

**Figure S4.**  $^{13}\text{C}$  NMR spectrum of compound **1**.

**Figure S5.**  $^{13}\text{C}$  NMR spectrum of compound **2**.

**Figure S6.** GPC overlay graph of compound **2**.

**Figure S7.** MALDI-TOF mass spectrum of compound **1**.

**Scheme S1.** Fragmentation pattern in compound **1**.

**Table S1.** Cell parameters of organotin DDSQs (compound **1** and **2**) obtained by DFT optimization.

**Table S2.** Comparison of selected DFT optimized geometrical parameters for the compound **1** and **2** with the corresponding experimental single crystal data.

**Figure S8.** DFT optimized unit crystal structure of compound **1** (left) and **2** (right) viewed along  $b$  vector direction.

**Figure S9.** Intermolecular  $\text{C-H}\cdots\pi$  and  $\text{C-H}\cdots\text{O}$  interactions in compound **1**.

**Figure S10.** Experimental and simulated PXRD patterns for (a) compound **1** and (b) compound **2**.

**Figure S11.** ADPs of compound **1** and **2**.

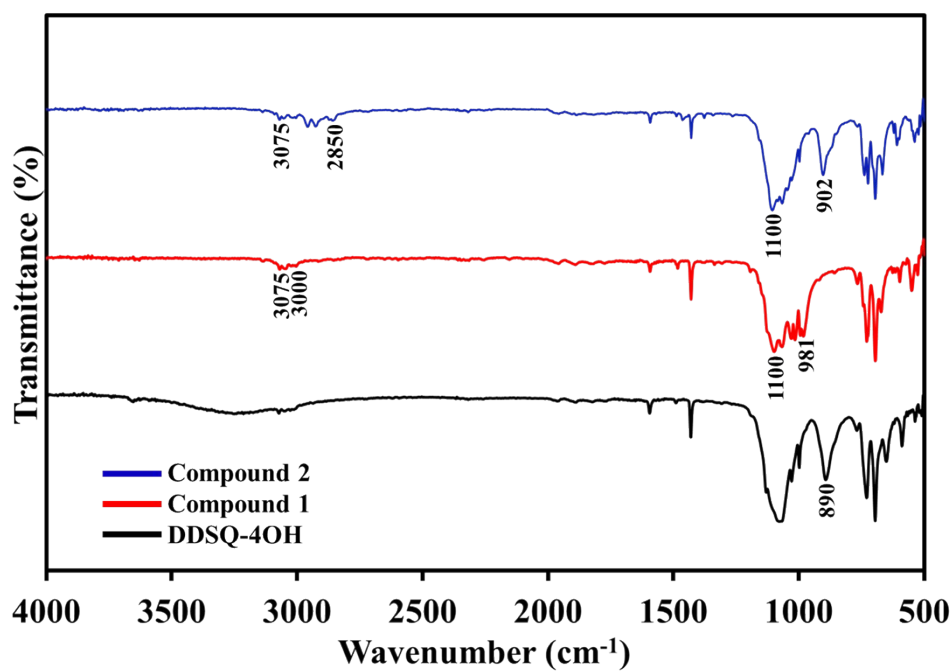


Figure S1. FT-IR spectra of DDSQ-4OH, compound 1 and 2.

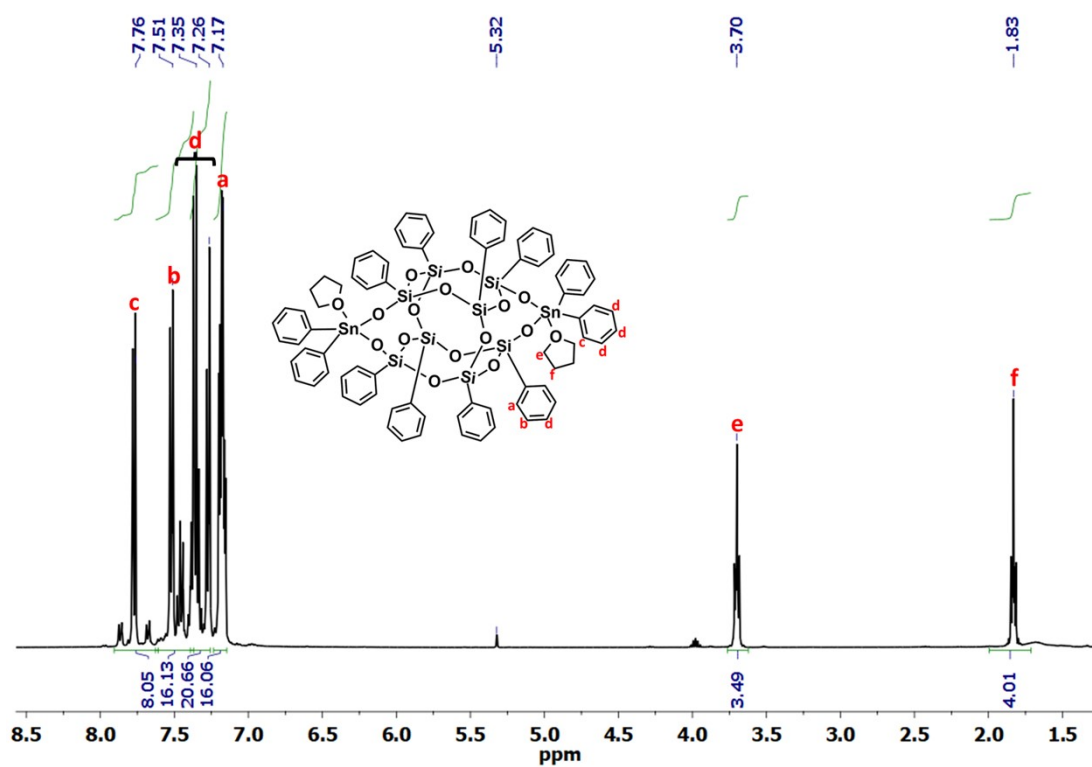


Figure S2. <sup>1</sup>H NMR spectrum of compound 1.

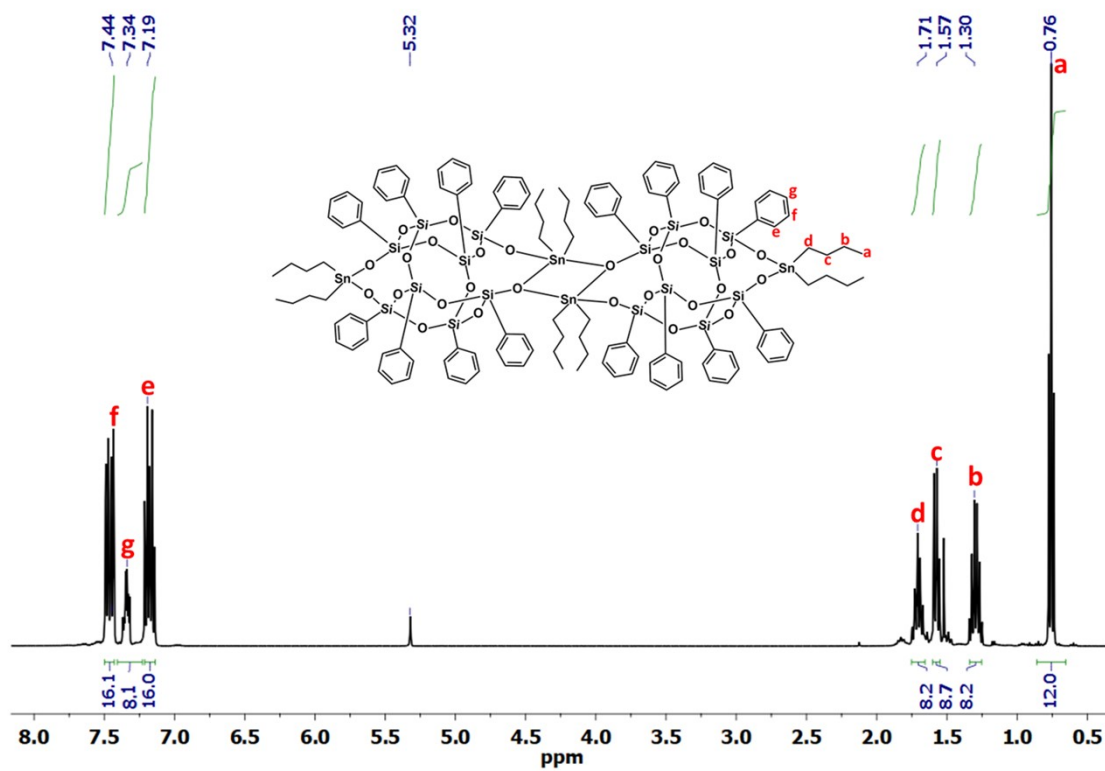


Figure S3.  $^1\text{H}$  NMR spectrum of compound 2.

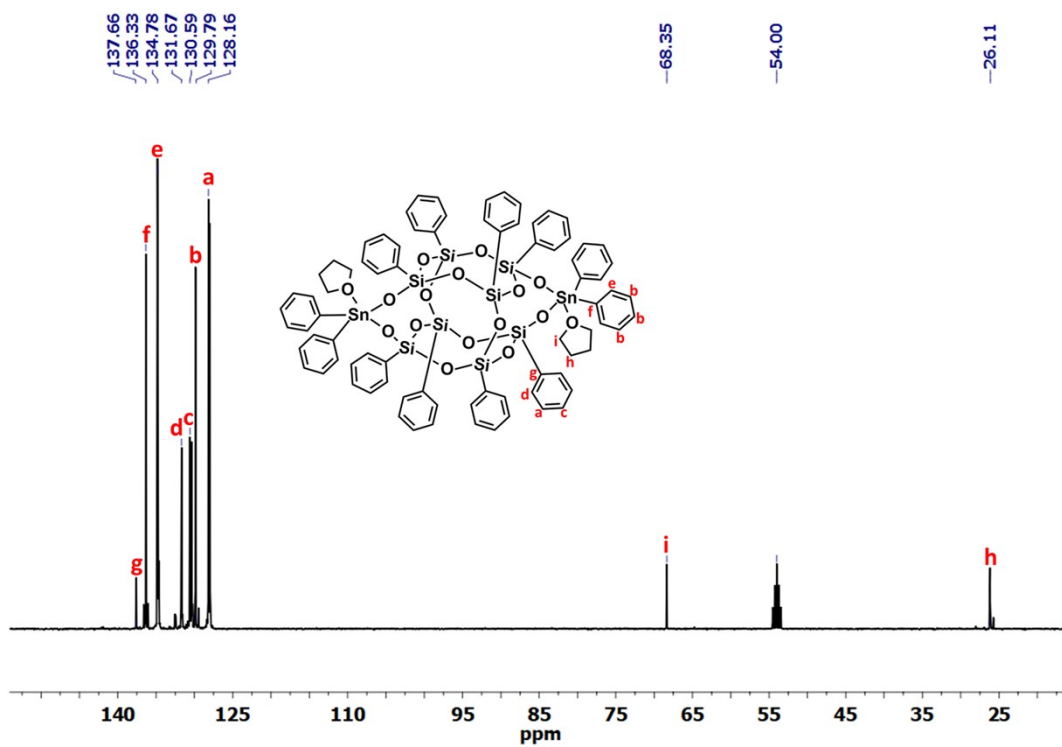


Figure S4.  $^{13}\text{C}$  NMR spectrum of compound 1.

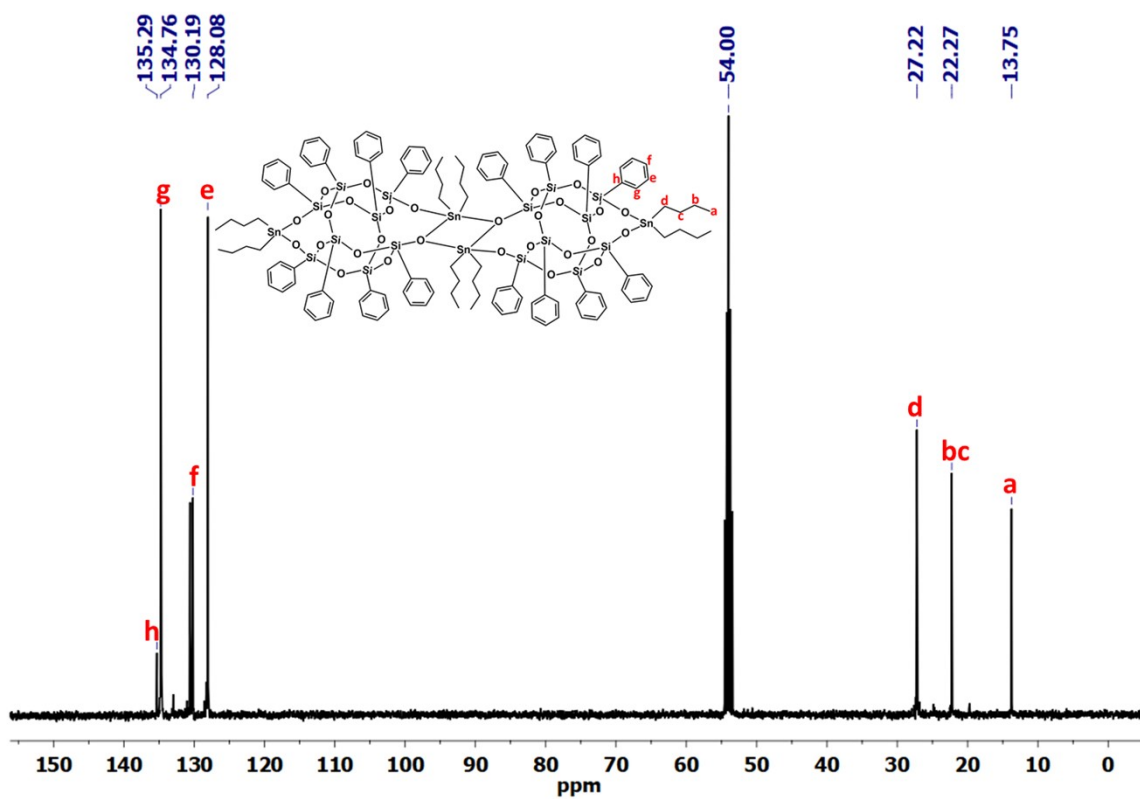


Figure S5.  $^{13}\text{C}$  NMR spectrum of compound 2.

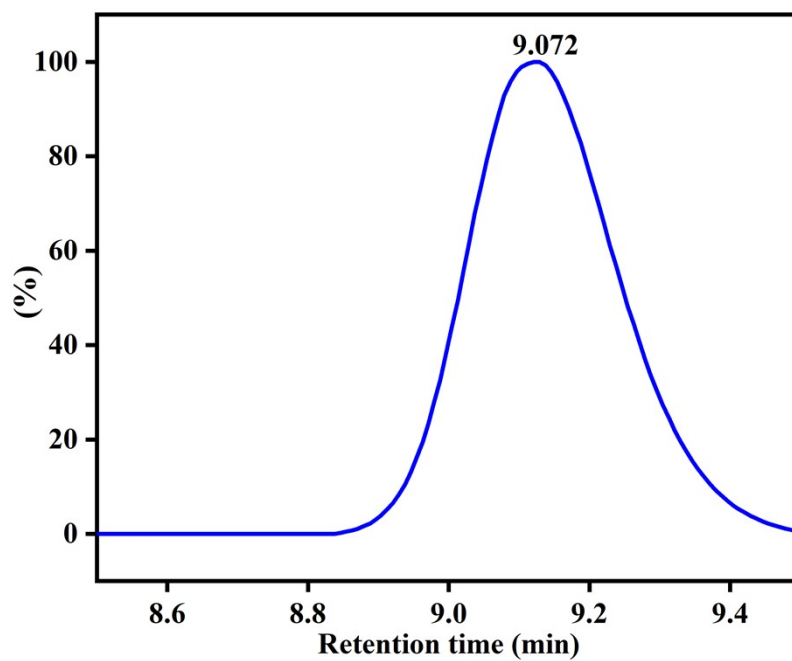


Figure S6. GPC overlay graph of compound 2.

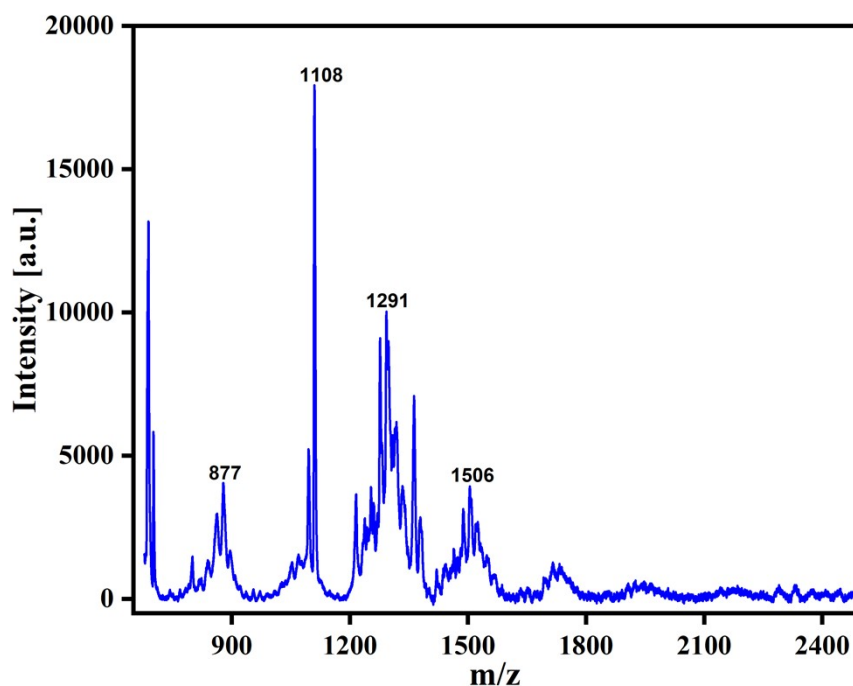
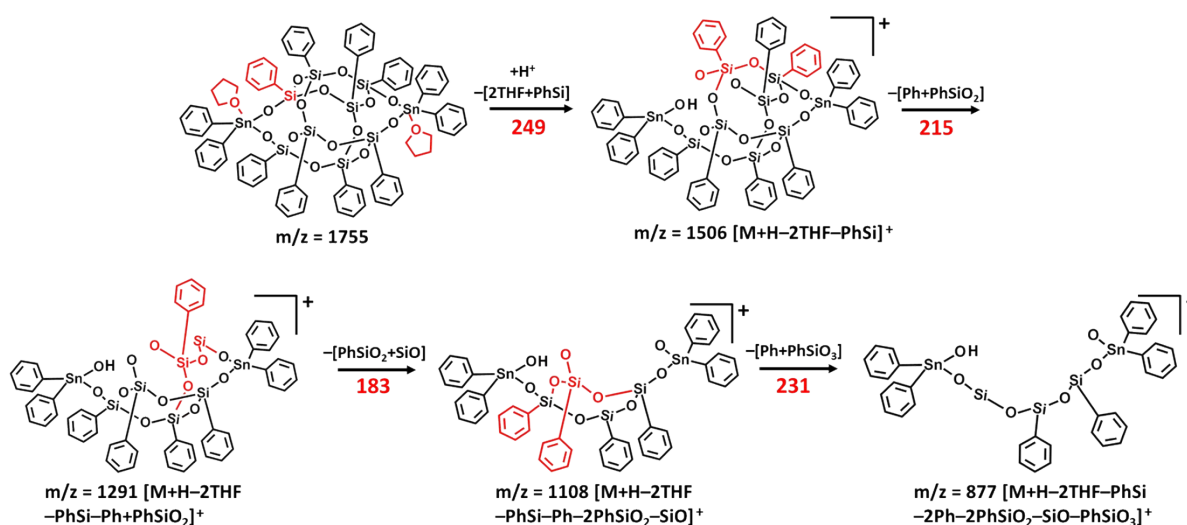


Figure S7. MALDI-TOF mass spectrum of compound 1.



Scheme S1. Fragmentation pattern in compound 1.

### Single crystal X-ray diffraction studies

A BRUKER Quest X-ray (fixed-Chi geometry) diffractometer with a PHOTON II detector was employed for crystal screening, unit cell determination, and data collection. The goniometer was controlled using the APEX3 software suite.<sup>1</sup> The sample was optically

centered with the aid of a video camera such that no translations were observed as the crystal was rotated through all positions. The X-ray radiation employed was generated from a Mo- $\mu$ s X-ray tube ( $K_{\alpha} = 0.71073\text{\AA}$ ). Integrated intensity information for each reflection was obtained by reduction of the data frames with the program APEX3.<sup>1</sup> The integration method employed a three dimensional profiling algorithm and all data were corrected for Lorentz and polarization factors, as well as for crystal decay effects. Finally the data was merged and scaled to produce a suitable data set. The absorption correction program SADABS was employed to correct the data for absorption effects.<sup>2</sup> A solution was obtained readily ( $Z=4$ ;  $Z'=0.5$ ) using XT/XS in APEX3.<sup>1,3</sup> Hydrogen atoms were placed in idealized positions and were set riding on the respective parent atoms. All non-hydrogen atoms were refined with anisotropic thermal parameters. Appropriate restraints and constraints were added to keep the bond distances, angles, and thermal ellipsoids meaningful. Absence of additional symmetry and voids were confirmed using PLATON (ADDSYM). The structure was refined (weighted least squares refinement on  $F^2$ ) to convergence.<sup>3,4</sup>

**Selected bond lengths [ $\text{\AA}$ ] and angles [ $^{\circ}$ ] of compound (1):**

Sn(1)–O(5) 1.995(2), Sn(1)–O(6) 1.966(1), Sn(1)–O(8) 2.546(2), Sn(1)–O(8A) 2.546(2), Si(1)–O(1) 1.623(2), Si(1)–O(2) 1.624(2), Si(1)–O(6) 1.606(1), Si(2)–O(2) 1.612(1), Si(2)–O(3) 1.605(1), Si(2)–O(7) 1.613(2), Si(3)–O(1)#1 1.608(1), Si(3)–O(3) 1.602(1), Si(3)–O(4) 1.612(2), Si(4)–O(4) 1.633(2), Si(4)–O(5) 1.585(2), Si(4)–O(7)#1 1.629(2), O(5)–Sn(1)–O(8) 172.29(6), O(5)–Sn(1)–O(8A) 172.29(6), O(6)–Sn(1)–O(5) 93.52(6), O(6)–Sn(1)–O(8) 79.09(6), O(6)–Sn(1)–O(8A) 79.09(6), O(1)–Si(1)–O(2) 109.49(8), O(6)–Si(1)–O(1) 110.71(8), O(6)–Si(1)–O(2) 110.88(8), O(2)–Si(2)–O(7) 110.58(8), O(3)–Si(2)–O(2) 108.83(8), O(3)–Si(2)–O(7) 109.95(8), O(1)#1–Si(3)–O(4) 109.91(8), O(3)–Si(3)–O(1)#1 110.69(7), O(3)–Si(3)–O(4) 109.34(8), O(5)–Si(4)–O(4) 109.85(9), O(5)–Si(4)–O(7)#1 111.66(9), O(7)#1–Si(4)–O(4) 107.51(8), Si(3)#1–O(1)–Si(1)

145.2(1), Si(2)–O(2)–Si(1) 155.2(1), Si(3)–O(3)–Si(2) 175.3(1), Si(3)–O(4)–Si(4) 145.5(1), Si(2)–O(7)–Si(4)#1 141.2(1), Si(4)–O(5)–Sn(1) 145.13(9), Si(1)–O(6)–Sn(1) 130.23(8).

**Selected bond lengths [Å] and angles [°] of compound (2):**

O(1)–Si(2) 1.604(3), O(1)–Si(3) 1.625(3), O(2)–Si(2) 1.603(4), O(2)–Si(4)#1 1.613(3), O(3)–Si(1) 1.603(3), O(3)–Si(2) 1.607(4), O(4)–Si(1) 1.593(4), O(4)–Si(3)#1 1.619(4), O(5)–Si(1) 1.610(3), O(5)–Si(4) 1.619(3), O(6)–Si(4) 1.604(3), O(7)–Si(3) 1.560(4), Si(3)–O(4)#1 1.619(4), Si(4)–O(2)#1 1.613(3), O(6)–Sn(1) 2.026(3), O(6)–Sn(1)#2 2.549(3), O(7)–Sn(1) 1.995(4), Sn(1)–O(6)#2 2.549(3), Si(2)–O(1)–Si(3) 149.6(2), Si(2)–O(2)–Si(4)#1 147.1(2), Si(1)–O(3)–Si(2) 154.7(2), Si(1)–O(4)–Si(3)#1 156.0(2), Si(1)–O(5)–Si(4) 144.1(2), Si(4)–O(6)–Sn(1) 129.9(2), Si(4)–O(6)–Sn(1)#2 125.6(2), Sn(1)–O(6)–Sn(1)#2 105.12(1), Si(3)–O(7)–Sn(1) 157.2(2), O(4)–Si(1)–O(3) 111.2(2), O(4)–Si(1)–O(5) 110.3(2), O(3)–Si(1)–O(5) 108.2(2), O(1)–Si(2)–O(2) 110.0(2), O(1)–Si(2)–O(3) 111.3(2), O(2)–Si(2)–O(3) 107.97(2), O(7)–Si(3)–O(4)#1 110.3(2), O(7)–Si(3)–O(1) 111.2(2), O(4)#1–Si(3)–O(1) 107.3(2), O(6)–Si(4)–O(2)#1 109.9(2), O(6)–Si(4)–O(5) 108.8(2), O(2)#1–Si(4)–O(5) 111.1(2), O(7)–Sn(1)–O(6) 94.2(1), O(7)–Sn(1)–O(6)#2 169.1(1), O(6)–Sn(1)–O(6)#2 74.9 (2).

**DFT Calculations**

The experimentally elucidated structures of compound 1 and 2 were geometry optimized at the Density Functional Theory (DFT) level using the CP2K package.<sup>5</sup> In these simulations, the positions of atoms of the framework were relaxed while the unit cell parameters were kept fixed at the values determined experimentally. All the structural optimizations were done using Perdew-Burke-Ernzerhof (PBE) functional along with a combined Gaussian basis set and pseudo potential.<sup>6</sup> For Carbon, Oxygen, and Hydrogen, a triple zeta (TZVP-MOLOPT) basis set was considered, while a double zeta (DZVP-MOLOPT) was applied for silicon and tin.<sup>7</sup> The pseudo potentials used for all of the atoms



were those derived by Goedecker, Teter and Hutter.<sup>8</sup> The van der Waals interactions were taken into account via the use of semi-empirical dispersion corrections as implemented in the DFT-D3 method.<sup>9</sup> The final optimized structures were used to simulate their powder diffraction patterns in Materials Studio. The Simulated patterns were obtained using the Reflex powder diffraction module of the material studio.

**Table S1.** Cell parameters of organotin DDSQs (compound **1** and **2**) obtained by DFT optimization.

Organotin DDSQs	Lattice Size(Å)			Angle (°)			Cell volume(Å <sup>3</sup> )
	a	b	c	$\alpha$	$\beta$	$\gamma$	
Compound <b>1</b>	23.419	13.5736	24.9877	90.0	90.902	90.0	7942.11
Compound <b>2</b>	11.062	13.602	14.652	115.767	102.870	101.726	1818.98

**Table S2.** Comparison of selected DFT optimized geometrical parameters for the compound **1** and **2** with the corresponding experimental single crystal data.

	Compound <b>1</b>		Compound <b>2</b>	
	Experimental (Å)	Simulated (Å)	Experimental (Å)	Simulated (Å)
Bond distance				
Si-O(Si)	1.627	1.636	1.618	1.62
Si-O(Sn)	1.596	1.602	1.587	1.6
Sn-O	1.981	2.04	2.01	2.01
Sn-O(THF)	2.546	2.653	-	-
Sn-O( $\mu$ )	-	-	2.546	2.47
Bond angle	Experimental (°)	Simulated (°)	Experimental (°)	Simulated (°)
Si-O-Si	141.2–175.3	143.6–176.9	143.8–155.8	142.6–148.9
Sn-O-Si	130.2–145.1	127.2–142.4	125.9–157.1	126.8–154.29
Sn-O-Sn	-	-	105.3	106.2

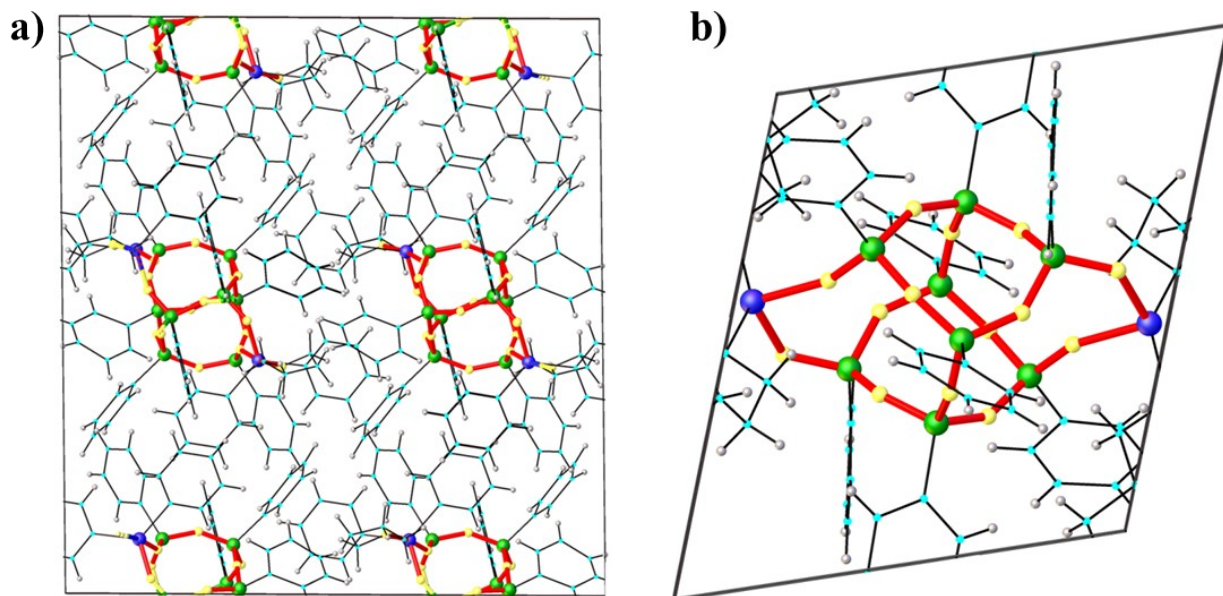


**Figure S8.** DFT optimized unit crystal structure of compound **1** (a) and **2** (b) viewed along *b* vector direction.

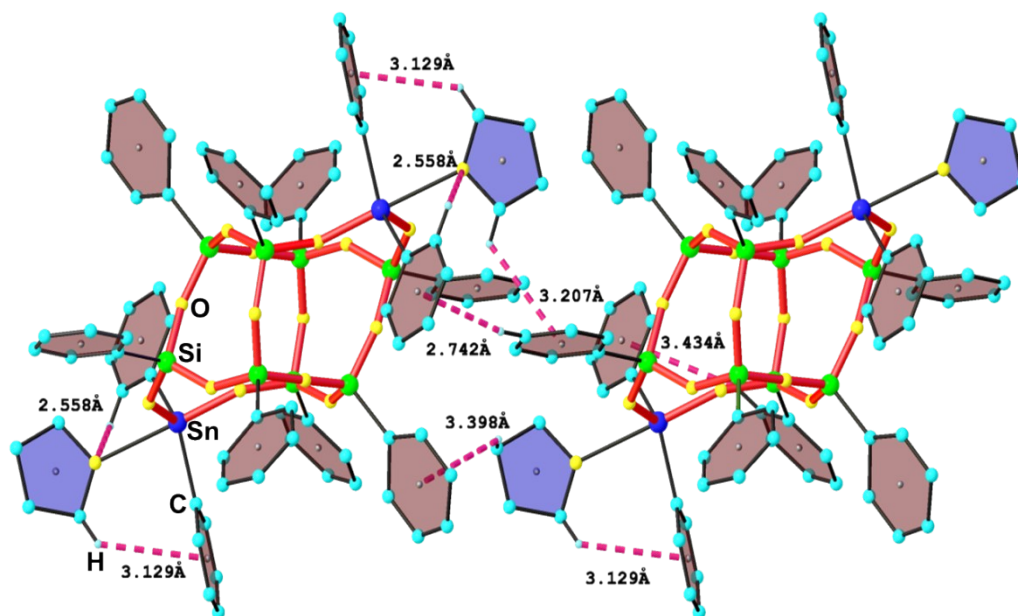


**Figure S9.** Intermolecular C–H $\cdots$  $\pi$  and C–H $\cdots$ O interactions in compound **1**.

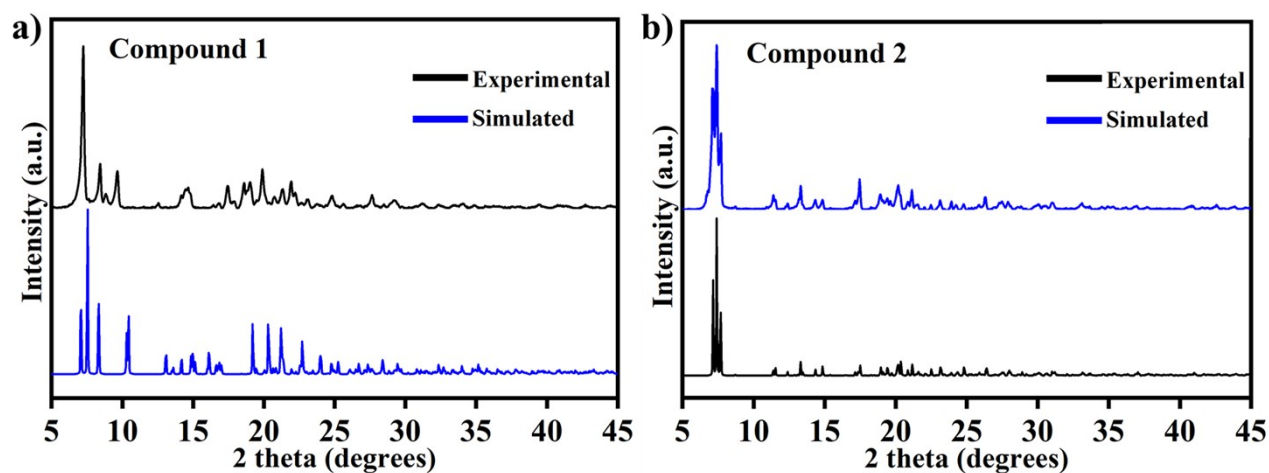


**Figure S10.** Experimental and simulated PXRD patterns for (a) compound 1 and (b) compound 2.

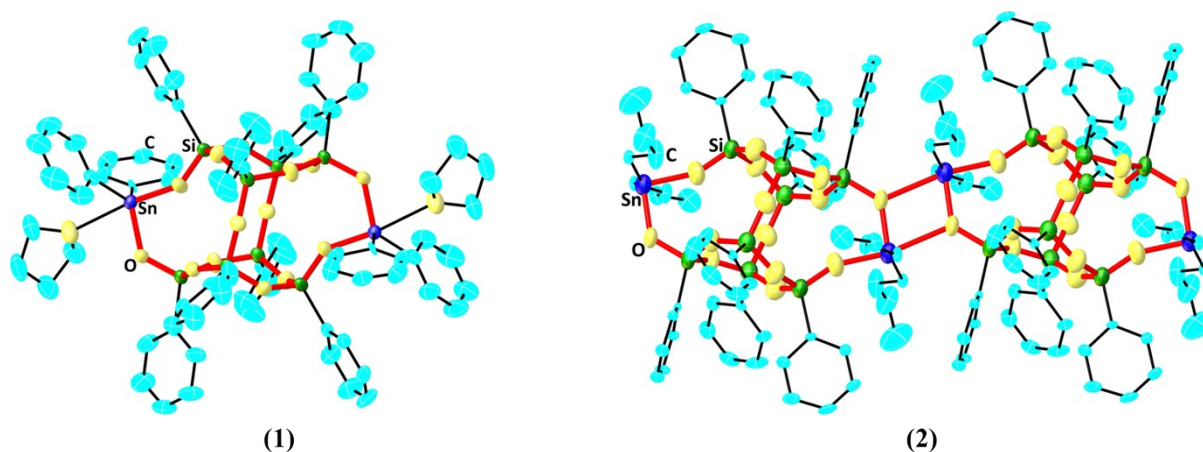


**Figure S11.** ADPs of compound 1 and 2.

## References

1. APEX3 “Program for Data Collection on Area Detectors” BRUKER AXS Inc., 5465 East Cheryl Parkway, Madison, WI 53711-5373 USA.
2. SADABS, Sheldrick, G.M. “Program for Absorption Correction of Area Detector Frames”, BRUKER AXS Inc., 5465 East Cheryl Parkway, Madison, WI 53711-5373 USA.

3. (a) G.M. Sheldrick, A short history of SHELX. *Acta Cryst.*, 2008, **A64**, 112-122; (b) G. M Sheldrick, SHELXT - Integrated space-group and crystal-structure determination. *Acta Cryst.*, 2015, **A71**, 3-8; (c) G. M. Sheldrick, Crystal structure refinement with SHELXL. *Acta Cryst.*, 2015, **C71**, 3-8.
4. O. V. Dolomanov, L. J. Bourhis, R. J. Gildea, J. A. K. Howard and H. Puschmann, *J. Appl. Cryst.*, 2009, **42**, 339-341.
5. T. D. Kühne, M. Iannuzzi, M. Del Ben, V. V. Rybkin, P. Seewald, F. Stein, T. Laino, R. Z. Khaliullin, O. Schütt, F. Schiffmann, D. Golze, J. Wilhelm, S. Chulkov, M. H. Bani-Hashemian, V. Weber, U. Borštnik, M. Taillefumier, A. S. Jakobovits, A. Lazzaro, H. Pabst, T. Müller, R. Schade, M. Guidon, S. Andermatt, N. Holmberg, G. K. Schenter, A. Hehn, A. Bussy, F. Belleflamme, G. Tabacchi, A. Glöß, M. Lass, I. Bethune, C. J. Mundy, C. Plessl, M. Watkins, J. VandeVondele, M. Krack and J. Hutter, *J. Chem. Phys.*, 2020, **152**, 194103(1)-194103(47).
6. (a) J. P. Perdew, *Phys. Rev. B*, 1986, **33**, 8822-8824; (b) J. P. Perdew, K. Burke and M. Ernzerhof, *Phys. Rev. Lett.*, 1996, **77**, 3865-3868.
7. J. Vande Vondele and J. Hutter, *J. Chem. Phys.*, 2007, **127**, 114105(1)-114105(9).
8. S. Goedecker, M. Teter and J. Hutter, *Phys. Rev. B.*, 1996, **54**, 1703-1710.
9. S. Grimme, J. Antony, S. Ehrlich and H. Krieg, *J. Chem. Phys.*, 2010, **132**, 154104(1)-154104(19).